Environmental Modelling and Software 115 (2019) 76–85

Contents lists available at ScienceDirect

Environmental Modelling & Software

journal homepage: www.elsevier.com/locate/envsoft

Bayesian inference of hydraulic properties in and around a white fir using a process-based ecohydrologic model

E.C. Massoud[a,b,*], A.J. Purdy[a,c], B.O. Christoffersen[d], L.S. Santiago[e], C. Xu[f]

[a] Jet Propulsion Laboratory, California Institute of Technology, Pasadena, CA, 91109, USA
[b] Department of Civil and Environmental Engineering, University of California, Irvine, Irvine, CA 92697, USA
[c] Department of Earth Systems Science, University of California, Irvine, Irvine, CA 92697, USA
[d] Department of Biology, University of Texas, Rio Grande Valley, TX, 78539, USA
[e] Department of Botany and Plant Sciences, University of California, Riverside, Riverside, CA 92521, USA
[f] Earth and Environmental Sciences Division, Los Alamos National Laboratory, Los Alamos, NM, 87544, USA

ARTICLE INFO

Keywords:
Ecohydrology
Vegetation
Hydraulics
Climate
Parameter estimation
MCMC

ABSTRACT

We present a parameter estimation study of the Soil-Tree-Atmosphere Continuum (STAC) model, a process-based model that simulates water flow through an individual tree and its surrounding root zone. Parameters are estimated to optimize the model fit to observations of sap flux, stem water potential, and soil water storage made for a white fir (*Abies concolor*) in the Sierra Nevada, California. Bayesian inference is applied with a likelihood function that considers temporal correlation of the model errors. Key vegetation properties are estimated, such as the tree's root distribution, tolerance to drought, and hydraulic conductivity and retention functions. We find the model parameters are relatively non-identifiable when considering just soil water storage. Overall, by utilizing multiple processes (e.g. sap flow, stem water potential, and soil water storage) during the parameter estimation, we find the simulations of the soil and tree water properties to be more accurate when compared to observed data.

1. Introduction

Ecohydrology is a field of study focusing on the hydrologic mechanisms that govern and explain ecologic patterns and processes (Rodriguez-Iturbe, 2000; Jackson et al., 2009). Ecohydrologic system properties depend on many interrelated links between climate, soil, and vegetation (Rodriguez-Iturbe et al., 2001). One part of this system includes the role that climate and soil have in controlling vegetation dynamics (Lange et al., 1976; Boyer, 1982; Kramer and Boyer, 1995; Larcher, 2003; Jones, 2013; Ali et al., 2016), and another part of the system is the control that vegetation exerts on the water and energy balance (Schlesinger et al., 1990; Kutzbach et al., Harrison; Zeng et al., 1999; Massoud et al., 2018a). A quantitative understanding of these vegetation dynamics better supports environmental preservation, management of resources, and improved model representation of ecohydrologic systems (Noy-Meir, 1973; Shmida et al., 1986; Scholes and Walker, 2004; Xu et al., 2013; Johnson et al., 2018).

Generally, the role that trees play in the overall water cycle in regards to ecosystem water storage, residence time, and vegetation tolerance to drought are poorly represented in Land Surface Models (LSMs) (Fisher et al., 2018). For example, the impact of soil water availability on vegetation is typically represented in land surface and climate models using simple empirical relationships, with parameter values that are extracted from arbitrary data sets. This may not represent vegetation hydraulic properties or capture seasonal or ontogenetic changes observed in reality, which can cause major bias in the representation of vegetation in this suite of models. The lack of proper representation of water dynamics in vegetation contributes to large discrepancies seen between various model simulations that run into the next century (Sitch et al., 2008; McDowell et al., Mackay et al.). New models are expected to better capture the vegetation response to water stress as they can be directly constrained by observations at the process level. Observational data sets have been collected to fill some of the gaps in our understanding of tree water dynamics, especially in temperate and Mediterranean ecosystems (Zweifel et al., 2007; West et al., 2008; West et al., 2012; Matheny et al., 2014; Pivovaro et al., 2016; Matheny et al., Curtis). Such studies can inform ecohydrologic models by enhancing their fidelity and guiding their development (Christoffersen et al., 2016; Feng et al., Thompson). Additionally, these models can be diagnosed to help further understand the ecohydrologic

* Corresponding author. Jet Propulsion Laboratory, California Institute of Technology, Pasadena, CA, 91109, USA
E-mail address: elias.massoud@jpl.nasa.gov (E.C. Massoud).

https://doi.org/10.1016/j.envsoft.2019.01.022
Received 3 May 2017; Received in revised form 18 January 2019; Accepted 30 January 2019
Available online 02 February 2019
1364-8152/

relationships, providing information on where and what type of additional observations are needed to re-develop the models (Perämäki et al., 2001; Hofstetter et al., 2005; Massoud et al., 2018b). Future development will enhance the ability of LSMs to predict individual tree processes such as drought tolerance or storage capacity and thus enhance the overall representation of vegetation's effect on the global water cycle (McDowell et al., 2013; Medlyn et al., 2016).

Studies dedicated to understanding ecohydrologic processes have been a topic of interest for decades (Sala and Lauenroth, 1982; Tyree, 1988; Christoffersen et al., 2016). Previous works have highlighted the differences between saturated and unsaturated flow (Aumann and Ford, 2002), improved on the representation of branch junctions (Schulte and Brooks, 2003), linked tree sap flow to stem growth (Steppe et al., 2006), modeled both xylem as well as phloem water fluxes (Lacointe and Minchin, 2008; Hölttä et al., 2009), improved prediction of xylem abscisic acid (ABA) concentrations by proper accounting of sap flow (Dodd et al., 2008), improved understanding of the effect of root system architecture for the enhancement of drought tolerance (Draye et al., 2010), accounted for hydraulic redistribution between different soil parts via plant root systems (Prieto et al., 2012; David et al., 2013), provided a computationally efficient 1-D alternative to 3-D models that includes a xylem flow model (Janott et al., 2009), applied ecohydrologic models in a model emulation and machine learning framework (Massoud, 2019), among others.

We present here a Bayesian approach to estimate the parameters of a numerical model that simulates water storage and transport through a tree and its root zone, coined the Soil-Tree-Atmosphere Continuum (STAC) model. Several early papers have applied the Bayes' framework in tree transpiration models (Samanta et al., Ewers; Mackay et al., 2012; Rings et al., 2013). The STAC model used in this study is structured with an axi-symmetrical 2D (or quasi-3D) representation of water flow through the combined soil-tree domain, where the soil is simulated as a separate domain from the tree itself. The model uses Richards' equation and Mualem-van Genuchten hydraulic functions from (Van Genuchten, 1980) and (Mualem, 1976) to characterize water storage and movement through both the soil and tree domains. We utilize Bayesian inference to obtain parameter posterior distributions that allow model simulations to fit closely with observations made for a mature white fir (*Abies concolor*) in the Kings River Experimental Watershed (KREW) in the Sierra Nevada, California.

Our goals for this study are: to accurately simulate the dynamics of water flow in a single mature tree and its root zone (G1); to properly infer model parameters that dictate how much water can be stored (capacity) or can flow (conductance) in the tree and its surrounding soil domain (G2); and to assess the efficiency of parameter estimation based on the combination of different data sources (G3). Through this study we aim to diagnose some flaws or drawbacks of the model, while also highlighting the properties that are well-represented. Ordinarily parameter values used in model simulations do not accurately describe the underlying vegetation properties they are supposed to represent, and here we aim to estimate these parameter values along with their associated uncertainties. In this study, we will gauge the effect of the different data sources on the respective parameter estimation results.

2. Materials and methods

To estimate the parameter uncertainty of the STAC model, we apply Bayes' theorem within in a Markov Chain Monte Carlo (MCMC) framework (Katz, 2002). Numerical implementation of this application requires the user to specify a prior parameter distribution as well as a likelihood function. The prior distribution should encode all the subjective knowledge about the parameters before collection of the data, whereas the likelihood function summarizes, in a probabilistic sense, the compatibility of the observed data to the simulated model outputs. Likelihood functions play a key role in statistical inference, and here we utilize a specially designed likelihood function that can combine various data streams from several processes being considered. It is generally assumed that if only one data set is used for the parameter estimation, the parameter values will be fitted to that specific process too closely. However, by considering various processes during the parameter estimation, the parameter search will be balanced by each data set and an overall more realistic representation of the system properties can be achieved (Medlyn et al., 2015). To this end, we use the likelihood function defined in (Schoups and Vrugt) and utilize multiple processes during the parameter estimation. We show that this does provide an overall accurate estimation of the soil and tree water properties when compared to observed data.

2.1. STAC model

The Soil-Tree-Atmosphere Continuum (STAC) Model is a physically-based nonlinear modeling framework (Kumagai, 2001; Bohrer et al., Katul; Chuang et al., 2006; Mirfenderesgi et al., 2016), typical for the simulation of water flow in unsaturated media (Siqueira et al., Porporato; Rings et al., 2013). The STAC model discretizes the system domain and couples the soil with the tree domain, simulating the soil, roots and tree trunk as a continuum. Water flow is driven by water potential gradients along the coupled system (Bittner et al., 2005) with spatially distributed root water uptake and canopy transpiration sink terms. The STAC model utilizes the HYDRUS model for simulation of hydrodynamics (Simunek et al., 2008), where water flow through the soil and the tree root system and stem is driven by the evaporative demand and soil-available water, leading to a gradient in soil and xylem water potentials along the STAC. We approximate both the soil and plant conducting tissues by a porous medium, with conductive and capacitive properties that are a function of water potential.

2.2. Domain boundaries

HYDRUS allows the estimation of water potential, volumetric water content, and water flux density across the coupled soil-tree domain. Both the soil and tree trunk are modeled as axial-symmetrical, represented by a rectangular domain (Fig. 1) The simulated soil domain extends to 5 m outwards; three soil layers characterize the top 2.5 m in the unsaturated soil, and the bottom 2.5 m interval represents the weathered low conductivity saprolite that can store water but is inaccessible to tree roots.

The lower boundary of the soil at the 5 m depth was described by a seepage boundary, allowing water to leave the soil domain when saturated, and allowing for both upwards and downwards flow across the whole soil domain. The upper boundary of the soil domain consists of measured values of rainfall and evapotranspiration. The lower boundary condition of the tree trunk is root water uptake from the soil domain, and the upper boundary of the tree is atmospheric demand of potential evapotranspiration. The 10 cm radius of the tree trunk was chosen so that the domain volume is approximately equal to that of the sapwood of the tree.

We use observations of soil moisture, soil water retention curves, and assume hydraulic equilibrium to initiate water potential distribution across the domain. For the soil, we converted 24 elements of soil moisture data collected on July 15, 2009, to soil water matric potential values using the laboratory-measured retention curves. Then, a 2nd order polynomial interpolation scheme was applied to estimate the soil water potential across the measured soil domain, assuming hydraulic equilibrium at the domain boundaries. This completed the necessary initial and boundary conditions of the domain for the model simulations.

2.3. Unifying equations

To set up the model simulations, we use the finite element HYDRUS software (Simunek et al., 2008), which can solve unsaturated water

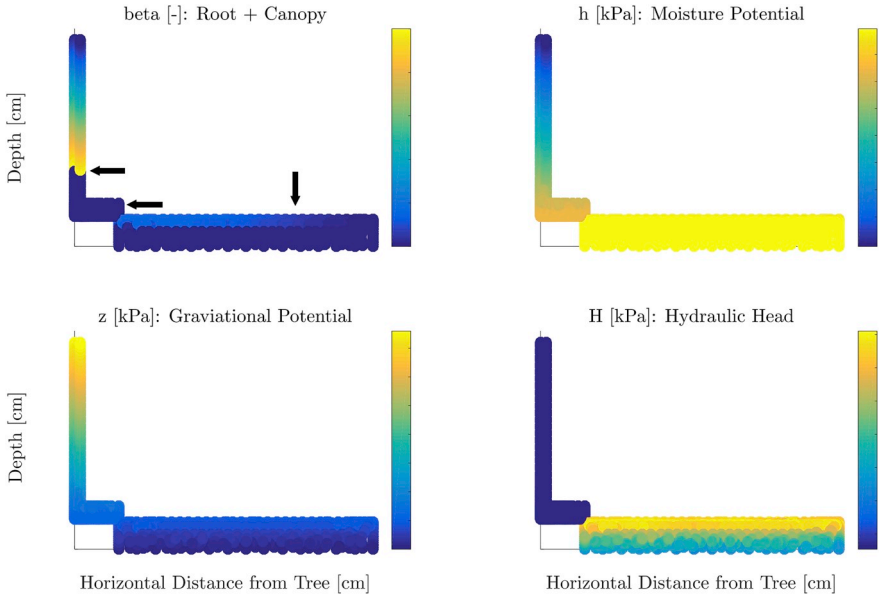

Fig. 1. Initial domain used in the STAC model simulations. 'beta' represents the root or canopy distributions in Equations (7) and (13).

flow across the soil-tree domain using the Richards' Equation (Richards, 1931) in a discretized system of linear equations (Equations (1) and (2)). The flow in the soil domain is presented here in its axisymmetrical, two-dimensional, isotropic form:

$$\frac{\partial \theta_{\text{Soil}}}{\partial t} = \frac{1}{r}\frac{\partial}{\partial r}\left(rK_r(h)\frac{\partial h}{\partial r}\right) + \frac{\partial}{\partial z}\left(K_z(h)\frac{\partial h}{\partial z}\right) - \frac{\partial K_z(h)}{\partial z} - W_{\text{Soil}}(h, r, z) \quad (1)$$

where θ_{Soil} (L^3L^{-3}) is the volumetric soil water content, $K(h)$ (LT^{-1}) defines the unsaturated hydraulic conductivity function (further denoted by either *r*-for radial direction or *z*-for vertical direction), h (L) is the soil water pressure head, r and z are the lateral and vertical coordinates (positive downwards) of the soil domain respectively, t (T) is time, and W_{Soil} ($L^3L^{-3}T^{-1}$) defines a sink/source term that quantifies spatially distributed root water uptake from the soil. Both K and W_{Soil} are functions of θ and/or h. The subscripts *r*- and *z*-allow for the possibility of soil anisotropy, i.e., to simulate water flow with the unsaturated hydraulic conductivity function being different for the *r*- and *z*-directions.

The set up of Richards' equation for the tree domain to represent flow through the canopy is similar to that of the soil domain in Equation (1), but in one-dimensional form. This equation is derivable directly from Equation (1) by reducing to one dimension, *z*-only. Thus, the axisymetrical flow through the tree canopy is represented by:

$$\frac{\partial \theta_{\text{Tree}}}{\partial t} = \frac{\partial}{\partial z}\left(K_z(h)\frac{\partial h}{\partial z}\right) - \frac{\partial K_z(h)}{\partial z} - W_{\text{Tree}}(h, z) \quad (2)$$

where θ_{Tree} (L^3L^{-3}) is the volumetric soil water content, $K(h)$ (LT^{-1}) defines the unsaturated hydraulic conductivity function (further denoted by *z*-for vertical direction), h (L) is the soil water pressure head, z is the vertical coordinate of the tree domain (positive downwards), t (T) is time, and W_{Tree} defines a sink term ($L^3L^{-3}T^{-1}$) that quantifies spatially distributed canopy transpiration.

For solution of Equations (1) and (2), unsaturated hydraulic conductivity and the water retention functions must be defined for both the soil and tree conducting matrix. The unsaturated hydraulic conductivity function (Equation (3)) defines the relationship between the moisture content and the corresponding hydraulic conductivity of the domain, and the retention function (Equation (4)) characterizes the ability of the domain to retain water. We define these functions using the relationships of (Van Genuchten, 1980) and (Mualem, 1976), where

$$K(h) = K_S\sqrt{S_{eff}}\left(\left(1 - \left(1 - S_{eff}^{\frac{1}{m}}\right)^m\right)^2\right). \quad (3)$$

and

$$S_{eff}(h) = \frac{\theta - \theta_r}{\theta_s - \theta_r} = (1 + |\alpha h|^n)^{-m}. \quad (4)$$

in which $K(h)$ represents the hydraulic conductivity, and the degree of effective saturation, $S_{eff}(h)$ represents the retention function. For these equations, θ_s denotes the saturated water content at $h = 0$ (L^3L^{-3}), θ_r is the residual water content (L^3L^{-3}), α is a scale parameter inversely proportional to mean pore diameter (L^{-1}), n ($m = 1–1/n$) is a shape parameter of the soil water characteristic, and K_S (LT^{-1}) is the conductivity at saturated conditions, or when $\theta = \theta_s$.

2.3.1. Root water uptake model

The actual root water uptake term in Equation (1) is computed from:

$$W_{\text{Soil}}(h, r, z) = \gamma(h)\beta(r, z)\pi r_m^2 T_p. \quad (5)$$

with $W_{\text{soil}}(h, r, z)$ representing actual water uptake of roots from the soil ($L^3L^3T^{-1}$) at each node in the soil domain, controlled by root density distribution, $\beta(r, z)$ (L^{-3}), and a soil water stress response function, $\gamma(h)$. r_m is a coefficient that represents the maximum radial root depth, and T_p is the potential tree transpiration shown later in Equation (9). Both $\beta(r, z)$ and $\gamma(h)$ have functional values between 0 and 1.

The normalized root distribution, $\beta(r, z)$ for an axisymmetrical soil domain Ω, is defined by (Vrugt et al., 2001; Gardenass et al., 2005):

$$\beta(r, z) = \frac{\beta^*}{2\pi\int_\Omega \beta^* d\Omega}. \cup \quad (6)$$

with a general nonuniform root distribution, β^*, as defined by (Vrugt et al., 2001):

$$\beta^*(r, z) = \left[\left(1 - \frac{z}{z_m}\right)\right]\left[\left(1 - \frac{r}{r_m}\right)\right]e^{-\left(\frac{p_z}{z_m}|z^* - z| + \frac{p_r}{r_m}|r^* - r|\right)} \quad (7)$$

where z_m and r_m define the maximum rooting extent in the vertical and radial directions (L), respectively. z^* and r^* are empirical parameters (L) that shift the maximum of the distribution in vertical and radial direction, respectively, and p_z and p_r are empirical parameters that determine the exponential shape of the distribution.

For water-stressed root conditions in the soil, $\gamma(h)$ (dimensionless)

was introduced by (Feddes et al., 1978), and reduces root water uptake from its maximum possible value because of soil water stress. $\gamma(h)$ is defined by four water potential values, P1 through P4 (Feddes et al., 2001). For soil water potential values between P2 and P3, $\gamma(h)$ will be optimum and equal to 1.0. For h-values between P1 and P2 (soil aeration stress) and between P3 and P4 (soil water stress), $\gamma(h)$ values will be smaller than one and zero, at a minimum. The equation that describes the soil water stress response, $\gamma(h)$, as a function of water potential, h, in cm is:

$$\gamma(h) = \frac{(h + 25cm)}{(\mathrm{P3} + 25cm)}; \; if \; P3 < h < P4. \tag{8}$$

For the estimation of the potential tree transpiration (T_p) in Equation (5), meteorological data from a local weather tower were used to estimate local hourly potential evapotranspiration, ET_0, using the Penman-Monteith equation (Allen et al., 1998). This is the reference Penman-Monteith equation (as in (Allen et al., 1998)) where the surface/stomatal conductance parameters are for non-water limiting conditions. Values for the aerodynamic resistance and bulk surface stomatal resistance terms were calculated according to FAO guidelines (Allen et al., 1998). To estimate the potential tree transpiration, T_p, we multiplied ET_0 with a tree coefficient, $s_{ET}0$ $(-)$, or

$$T_p = s_{ET_0} \mathrm{ET}_0 - E_S. \tag{9}$$

We assume soil water evaporation, E_s, to be negligible as canopy cover dominates the landscape and dry surface soil moisture conditions occurred throughout the study time period.

Finally, from integration of Equation (5) over the soil domain, the actual total root water uptake, R_a, (L T^{-1}) is computed from:

$$R_a = \frac{2\pi}{\pi {r_m}^2} \int_{\Omega} rW_{\mathrm{Soil}} \, d\Omega. \tag{10}$$

In the presented coupled domain, the volume of water taken up by the roots must now be transported in the conducting vessels (xylem) of the sapwood in the tree trunk. For that purpose, the coupled model includes a small storage reservoir that acts as a buffer for water transport between the soil and the tree. Finally, by defining a lower flux boundary condition for the tree domain, the tree's sapwood draws water from the buffer storage and initiates water flux through the tree. This water flux, and ultimately tree transpiration, are discussed in the next section.

2.3.2. Tree transpiration

The STAC model uses the Jarvis model to quantify plant transpiration (Waring et al., 1979). Specifically, the canopy transpiration sink term, $W_{\mathrm{tree}}(h, z)$, in Equation (2) is calculated as follows:

$$W_{\mathrm{Tree}}(h, z) = \gamma(h)\beta(z)T_p. \tag{11}$$

where $\beta(z)$ is the one-dimensional canopy density distribution function used for estimation of transpiration at different elevations along the canopy in the tree domain, $\gamma(h)$ is the canopy water stress response function that represents the stomatal closure under increasing water tension and is of a similar Feddes form as used for characterizing soil water stress. T_p is the potential tree transpiration from Equation (9).

The normalized canopy distribution, $\beta(z)$ for an axisymmetrical tree domain Ω, is defined by (Vrugt et al., 2001; Gardenass et al., 2005):

$$\beta(z) = \frac{\beta^*}{2\pi \int_{\Omega} \beta^* d\Omega}. \tag{12}$$

with a general nonuniform tree distribution, β^* (L^{-1}), as defined by (Rings et al., 2013):

$$\beta^*(z) = 1 - \left(\frac{z - 6}{24}\right). \tag{13}$$

for $z > 6$ m and zero below 6 m. In other words, the tree distribution term that controls transpiration is zero at heights of the tree trunk that are below 6 m, is at a maximum at 6 m, and decreases linearly with height at points above 6 m. Thus, the actual tree transpiration (T_a) is computed from:

$$T_a = \frac{2\pi}{\pi {r_m}^2} \int_{\Omega} rW_{\mathrm{Tree}} d\Omega = 2\pi R_a \int_{\Omega} \gamma(h)\beta(z) dz. \tag{14}$$

Overall, this approach couples root water uptake with tree transpiration. Therefore, the model is set up so that at each time step the amount of total water uptake from the tree's roots, R_a, is equivalent to the water flow leaving the soil domain into the buffer zone of the tree, and the tree's transpiration, T_a, is the flow of water leaving the tree. The tree water storage calculation can be estimated as the difference between the water flowing into (R_a) and out of (T_a) the simulated tree domain. The solutions to these equations are estimated through a finite element mesh with thousands of nodes dividing the domain of the problem into a collection of subdomains, with each subdomain represented by these sets of equations.

2.3.3. Sapflux and soil water storage

We can assume that the simulated values of the water fluxes and stores at each individual node in the finite element mesh grid represent the true values in the actual tree-soil system. This assumption allows for the calculation of processes such as sapflux or soil water storage at each time step. For calculation of the sapflux output, the STAC model simulates the change in water content at each node at each time step. This directly allows the simulation of water flux in the model, the amount of which is controlled by the chosen parameterization. The STAC model does not output soil water storage directly, yet by combining the water content information at each node, one can estimate the water storage changes at each time step. Therefore if we take the soil water storage measurement value at initialization to be our starting point for the simulated soil water storage, then we can estimate the change of moisture content values at each time step and therefore calculate the change in storage and thus the storage level at each time step.

2.4. Data

The model will be tested using data collected in and around a white fir (*Abies concolor*) in a 99 ha subcatchment (P301) of the King's River Experimental Watershed (KREW), as part of the Critical Zone Observatory (CZO-TREE 1) project. This site is located in the rain-snow transition zone of the southern Sierra Nevada mountain range in California at an elevation of 2018 m. Data include soil water content and water potential in 3 spatial dimensions in the root zone, tree stem water content and sap flux, canopy water potential, and atmospheric variables including: net radiation, air temperature, and humidity. Undisturbed soil samples were collected to a depth of 2.5 m for the soil analysis. Corresponding measurements of saturated hydraulic conductivity were made using the constant head method (Reynolds et al., 2002).

Calibration data was selected for a 17-day rainless period in summer of 2009, starting July 15, and includes sapflow, stem water potential, and soil water storage. Three sap flow sensors (TransfloNZ, Palmerston North, NZ) were installed into the sapwood at a trunk height of 2.5 m. Using the compensation heat pulse technique (Green and Clothier, 1988), average sap flux flow (L/T) was estimated at 30-min time intervals. Then, stem water potential measurements were taken from terminal shoots of the stems of lower tree branches, at approximately 6 m height. Seven measurements were taken during 24 h on July 21–22, 2009. Finally, Echo- 5 TE soil moisture sensors were installed at depths of 0.15 m, 0.30 m, 0.60 m and 0.90 m in each of 6 locations within a 5 m radius from the tree trunk. The sensors were calibrated in the laboratory (Kizito et al., 2008), from which it was determined that their accuracy is around 3% for a range of soils. Using all water content

measurements, average total soil water storage (m^3) was computed during the 17-day measurement period every half hour. However, only about half of the soil water storage data was used for the parameter estimation due to incomplete measurements on some days.

2.5. Bayesian inference of model parameters

We chose a total of 15 parameters from the STAC model to be estimated. A total of 4 parameters are used to characterize the spatial tree root distribution (see Table 1), and these include z^* and r^* from Equation (7), which are empirical parameters (m) that shift the maximum of the distribution in vertical and radial direction, respectively, and p_z and p_r are empirical parameters that determine the exponential shape of the distribution. Also, a total of 3 parameters are used to characterize the water stress response functions (see Table 1). Finally, a total of 8 parameters are used to characterize the hydraulic conductivity and retention of the entire coupled domain (see Table 1). These parameters include θ_s, K_s, α, and n for the tree layer, and θ_s and K_s for soil layers 1 and 2.

Bayes' law, or Bayes' rule, mathematically expresses the fundamental relationship between the prior, conditional, and posterior beliefs of the parameter values, in this case a 15-dimensional vector denoted by $\mathbf{x}$. This probability equation can be formalized as $P(\mathbf{x}|\mathbf{Y}) \propto L(\mathbf{x}|\mathbf{Y})$, where $P(\mathbf{x}|\mathbf{Y})$ signifies the posterior parameter distributions, and $L(\mathbf{x}|\mathbf{Y})$ represents the likelihood function. The model simulations are coupled with observed data, $\mathbf{Y}$, to estimate the posterior probability of the parameters using a rigorous Markov Chain Monte Carlo (MCMC) sampling algorithm, the Differential Evolution Adaptive Metropolis (DREAM) of (Vrugt, 2016; Vrugt and Massoud, 2018). The likelihood function used for the MCMC sampling can combine all three sources of information, i.e. the sapflow, stem water potential, and soil water storage, without being affected by the magnitude of error that is contributed from any of the individual sources. This likelihood function is applied as follows:

$$L(\mathbf{x}|\mathbf{Y}, \varphi, \sigma^2) = -\frac{1}{2}\sum_{j=1}^{3}\sum_{t=2}^{n_j}\left\{\frac{(e_{j,t}(\mathbf{x}) - \varphi e_{j,t-1}(\mathbf{x}))}{\sigma_{j,t}}\right\}^2. \quad (15)$$

where j distinguishes the various model outputs considered for the parameter estimation, $\mathbf{x}$ is the parameter set, $\mathbf{Y}$ is the observed data, φ is the temporal correlation of the residuals (with 30 min between each time step), and σ is the measurement error of the calibration data. $e_{j,t}(x)$ is the error of the model simulations for output j and a given parameter set $\mathbf{x}$. Therefore, we calculate a likelihood value from each considered output (i.e. $L(\mathbf{x}|\mathbf{Y}, \varphi, \sigma^2)_j$), and as Equation (15) indicates we sum the three likelihood values to obtain one overall 'probability' value.

For this study we examine various parameter estimation strategies. First, we fit the model simulations to individual data sources (i.e. sapflux, stem water potential, and soil water storage), and then fit the simulations to all three sources combined. In the first case, the model is calibrated to just the sapflux data, and Equation (15) is reduced to just one term, the likelihood obtained from the fit to the sapflux data; these results are assigned the 'SAP' acronym. For the second and third cases, the model is calibrated to the stem water potential and soil water storage data, respectively, and Equation (15) is similarly reduced to one term; these results are assigned the 'STEM' and 'STOR' acronyms, respectively. In the final case, the model is calibrated to all three data sets, and Equation (15) utilizes all three likelihood terms; these results are assigned the 'FULL' acronym. This final case highlights the ability of the likelihood function to combine various data streams by normalizing the prediction errors based on the observation error and combining the likelihood (or probability) from all three processes considered. For the parameter estimation runs, the measurement error values were defined as $\sigma_{Sap} = 1$ cm/day, $\sigma_{Stem} = 100$ kPa, and $\sigma_{Stor} = 0.05\ m^3$.

2.6. Numerical setup and CPU costs

Calculation of the STAC model involves solution of the partial differential equations (PDE) that are described in the previous sections. The time difference between each model output is $\delta t = 30$ min, and the temporal discretization of the PDE is based on an adaptive time step, limited by 10 maximum iterations and with tolerances of 0.01 (unitless) and 10 (kPa) to solve the moisture levels when described by the moisture content, θ, or the head, h, respectively. The spatial discretization is designed by a finite element mesh with thousands of nodes, and the location of these nodes for our case study are depicted in Figs. 1 and 3, with each dot representing the center of a node. This first involves dividing the domain of the problem into a collection of subdomains, with each subdomain represented by a set of element equations to the original problem, followed by systematically recombining all sets of element equations into a global system of equations for the final calculation.

The STAC model simulation time is 30 seconds on average for the 17-day period in the Sierra Nevada test site. For the MCMC runs, we used a total of 8 chains and ran for 2500 generations. Therefore a simple calculation shows that the STAC model parameters can be estimated in roughly 30 seconds multiplied by 8 chains multiplied by 2500 generations. This amounts to 600,000 seconds to apply the parameter estimation, which ultimately translates to a week of simulation time. For convergence of the posterior distributions, we noticed that the SAP and FULL strategies converged well into the 2500 generations. However, for the STEM strategy the posterior solution converged relatively quickly since there were only 7 measurements to fit against. Lastly, and importantly, for the STOR strategy the posterior solution was never really identified, even after 2500 generations.

3. Results

For the remainder of the paper, the results are color coded as follows: the estimation to sapflux (SAP) is shown in blue, estimation to stem water potential (STEM) is shown in light blue, estimation to soil water storage (STOR) is shown in green, and estimation to all three data sets (FULL) is shown in black.

3.1. Parameter estimates

The STAC model simulates the spatial root distribution of the tree using Equation (7). For the four estimation methods considered, the estimated root distribution parameters are shown in Table 1. The standard deviation of the posterior samples are shown in parenthesis in Table 1 and are represented graphically in Fig. 2. The resulting root distributions shown in Fig. 3 allow a visual comparison of all the different estimation strategies.

Both the tree and its roots may experience stress from water limitation, as well as nutrient limitation, or stress from extreme vapor pressure deficits as a result of hot temperatures, among other factors. The STAC model numerically accounts for this through the stress terms, γ, in Equations (5) and (11). These stress terms are characterized using the Feddes function ((Feddes et al., 1978)), and have values ranging from 0 (full stress) to 1 (no stress). Four levels of head, or pressure, are used to express this function, P1, P2, P3, and P4. For soil water potential values between P2 and P3, there is no stress, while the stress occurs between P1-P2 (aeration stress, or saturated conditions) and between P3-P4 (water stress, or drought conditions). A few of these coefficients are parameterized, and the calibrated values are shown in Table 1. The standard deviation of the posterior samples are shown in parenthesis in Table 1 and are represented graphically in Fig. 2. After all Feddes parameters are defined, the stress functions for each layer can be constructed. These functions are shown in Fig. 4 and also allow a visual comparison of the various estimation strategies.

Through Equations (3) and (4), the STAC model characterizes the

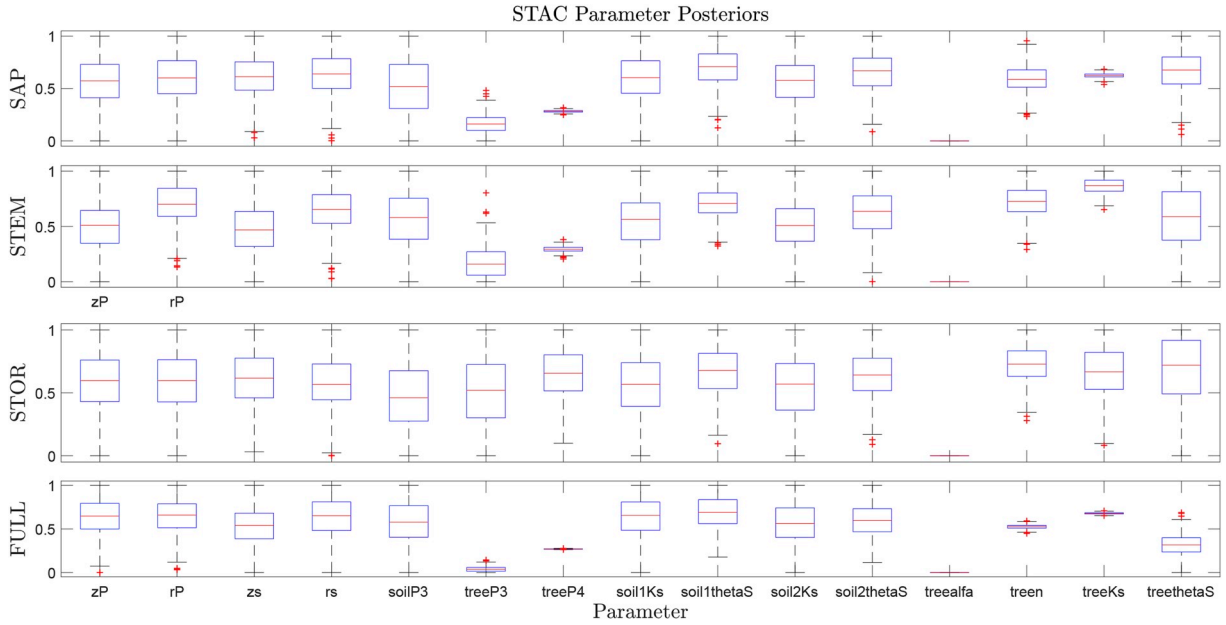

Fig. 2. STAC model parameter posterior distributions created from each of the considered strategies. Normalized ranges allow for better visualization of all parameter posteriors on the same plot. Posteriors represented with smaller box plots indicate a more localized posterior distribution, and thus a more informative one.

retention and hydraulic conductivity of each soil layer and of the tree layer. Table 1 shows the values of the model parameters that are van Genuchten parameters used to create hydraulic relationships of the tree and soil domains. The standard deviation of the posterior samples are shown in parenthesis in Table 1 and are represented graphically in Fig. 2. These parameters help represent the saturated conductivity and moisture contents of each layer and also contain certain shape parameters for the van Genuchten functions. The resulting hydraulic conductivity and retention functions for soil layers 1 and 2 as well as for the tree layer are shown in Fig. 5. In the first column of figures, the retention function of each layer is shown. One thing to note is that the retention function of the tree domain greatly differs from that of the soil layers. The figure shows that it will require higher amounts of pressure to extract the water from the tree than from the soils (-10^3 kPa for soils vs. -10^5 kPa for tree), which can be expected (North and Nobel, 1997; Black and Pritchard, 2002).

3.2. Comparing STAC model simulations with observations

In this study we focus on three processes represented in the STAC model, which are the sapflux through the tree domain, the stem water potential in the canopy, and the water storage of the soil domain. All of these outputs are accompanied by observed data, and the model simulation results are shown in Fig. 6 for each parameter estimation method. For the sapflux simulations, the SAP and FULL strategies performed the best according to the RMSE (Table 2). The other estimation strategies (STEM and STOR) do not fit the observations quite as well, however they do allow the simulations to capture high peaks in the observed data. For the stem water potential simulations, the STEM strategy provided the lowest RMSE. Although estimation to the stem water potential data was not as informative since there were only 7 data points to fit, these observations still allow us to constrain the simulations. This is shown in Table 2 since the RMSE for the stem water

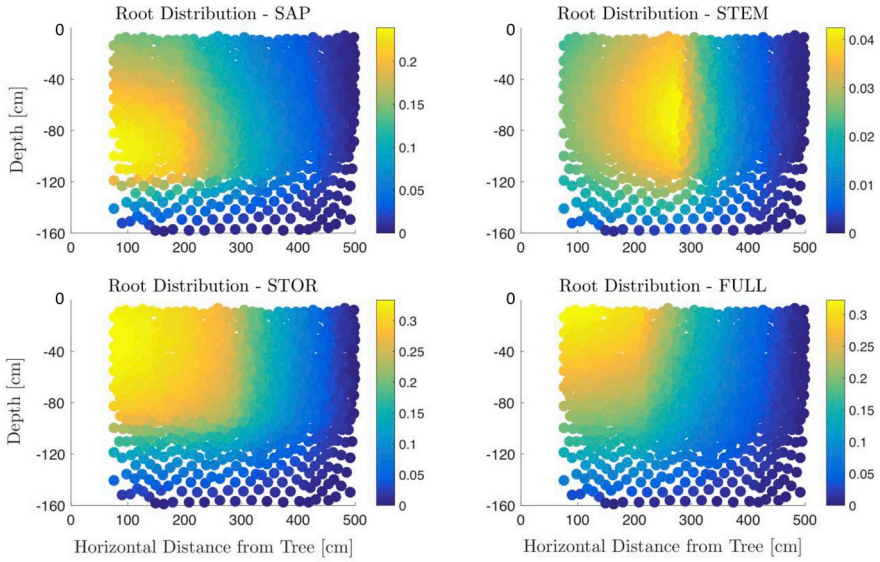

Fig. 3. Root distributions created from each of the parameter estimation methods. These figures were created using parameter values from Table 1 and the general nonuniform root distribution formula of Equation (7).

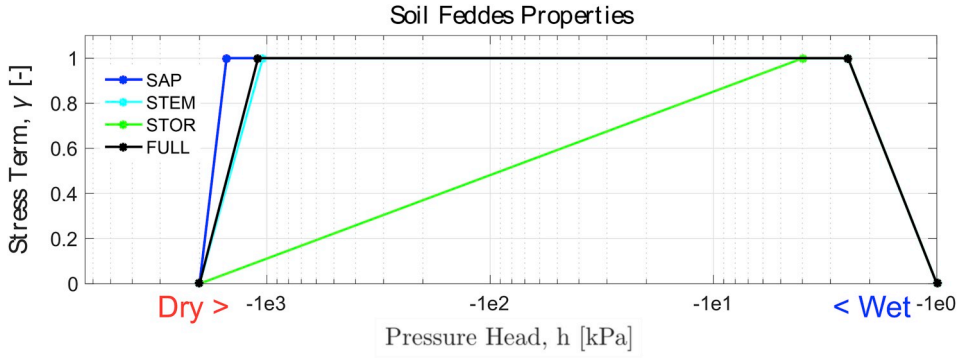

Fig. 4. Feddes stress functions for the soil layer. These functions were created using the coefficients of Table 1. The stress term, γ, in Equation (5) are the values on the y-axis. For pressure head values between P2 and P3, there is no stress and $\gamma = 1$. The stress occurs between P1-P2 (aeration stress, or saturated conditions) and between P3-P4 (water stress, or drought conditions). The various soil P3 values that were estimated with each MCMC strategy are. shown with a different color. (For interpretation of the references to color in this figure legend, the reader is referred to the Web version of this article.)

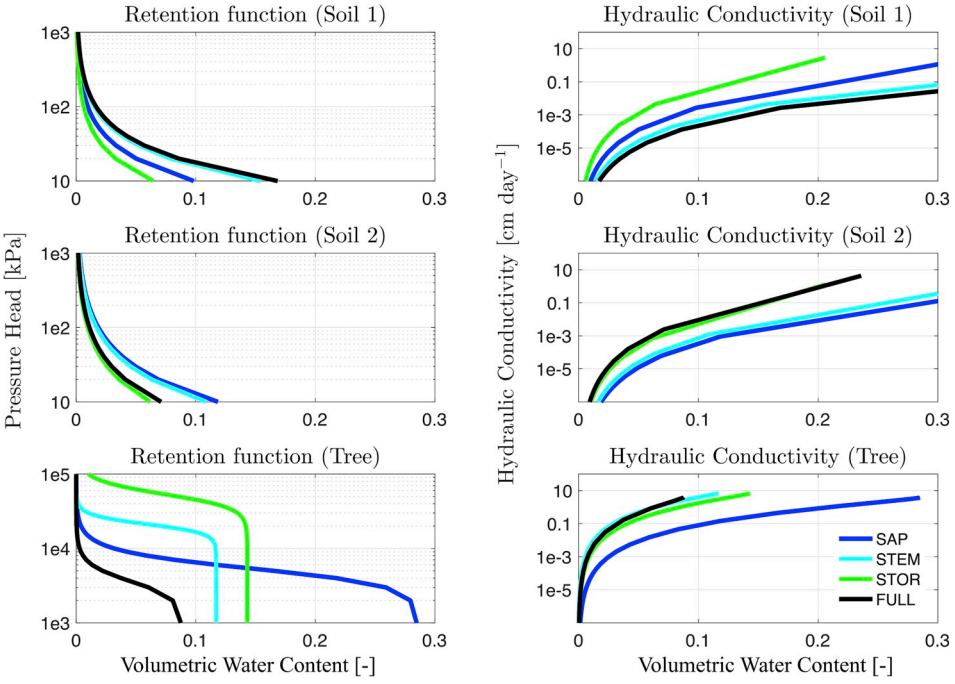

Fig. 5. Hydraulic relationships for soil layer 1, soil layer 2, and the tree layer. Shown in the first column of figures are the retention functions for each layer (with the y-axis being negative pressure head), and in the second column the hydraulic conductivity of each layer is shown. The parameters used to create these relationships are presented in Table 1.

potential simulations of the FULL strategy is lower than that of the SAP and STOR strategies, which is not surprising since the FULL strategy considers the stem water potential data in its likelihood function. For the soil water storage simulations, the STOR parameter set performed the best according to the RMSE, yet we see in Fig. 6 that all the simulations behave almost identically. In all simulations, the model underestimated the observed soil water storage, indicating a model structural error that could be from more water being drawn from the soil domain in the simulations than is seen in the observed data, or perhaps this could be due to the use of a likelihood function that only accounts for short-term temporal correlation.

4. Discussion

For this study we wanted to accurately simulate the dynamics of water flow in and around a mature white fir in the Sierra Nevada, California, using a process based ecohydrologic model, the STAC model (G1). To achieve these simulations, we inferred model parameters that dictated how much water can be stored or can flow in the tree and its surrounding soil domain (G2). Lastly, we combined various data sources to accurately pinpoint the posterior distributions for the model parameters (G3).

By fitting the observed data and its underlying uncertainty, we were able to mimic the dynamics seen for the white fir using the process based STAC model. Our results indicate that some STAC model parameters were not identifiable regardless of the data used for parameter estimation, such as the root distribution parameters. However, some parameters were estimated well, with posterior distributions that were well identified regardless of the data set used, such as the parameter that describes the tree's saturated hydraulic conductivity ($K_{s,Tree}$). Overall, as hypothesized, the combination of all three data sets allows for the most precise estimation of the model parameters, with the most localized posteriors and thus the least uncertainty about the corresponding parameter values.

In past parameter estimation studies, it has been common to separate data sets to calibrate the model on the first set of data and then to evaluate that calibration on the second set. However, given the lack of data availability for this study, such as only having 7 stem water potential measurements to use, this type of evaluation is challenging. Thus, in this study, we focus on parameter estimation to the observed data but leave model validation for future studies.

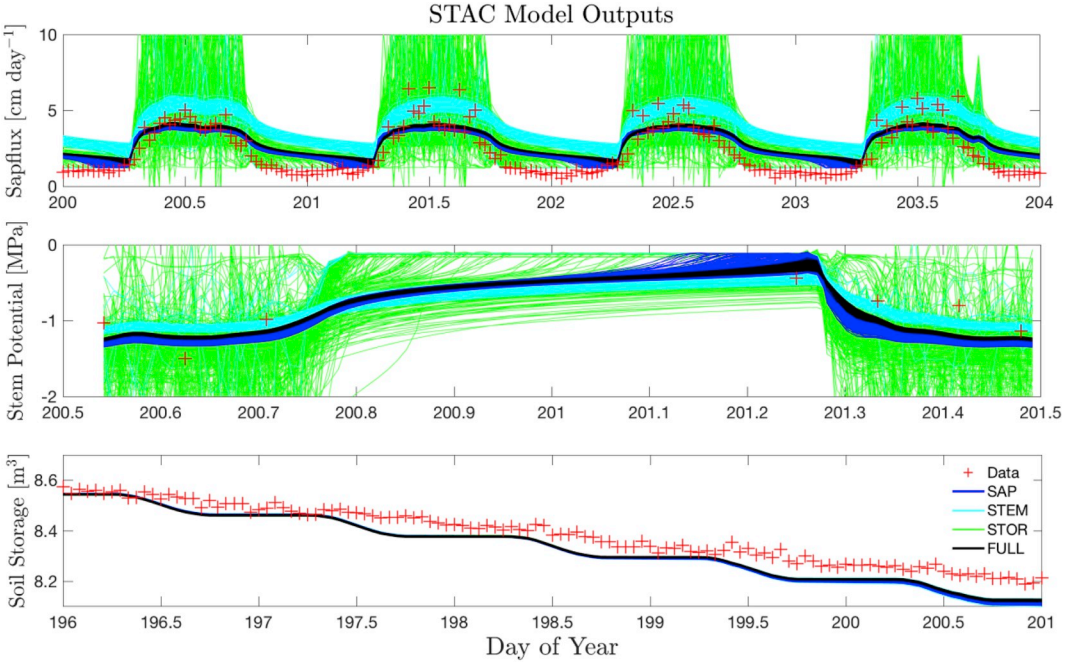

Fig. 6. Posterior solutions of the STAC model outputs, including sapux (cm day^{-1}), stem water potential (MPa), and water storage in the soil domain (m^3). Observations are shown with red marks. The simulations with parameters calibrated to sapflux data are shown in blue (SAP), simulations with parameters calibrated to stem water potential data are shown in light blue (STEM), simulations with parameters calibrated to soil water storage data are shown in green (STOR), and simulations with parameters calibrated to all the data are shown in black (FULL). (For interpretation of the references to color in this figure legend, the reader is referred to the Web version of this article.)

4.1. Model limitations

Interestingly, our results show that most of the parameters were not identifiable when just the soil water storage measurements were used as calibration data (STOR). The only parameters that showed any sensitivity to calibration of this output were the $\theta_{s,Soil1}$ and the α_{Tree} parameters. We can infer from the very wide posterior distributions for the STOR estimates (Fig. 2). This informs us that the soil water storage might very well be ill-represented in the model. Additionally, the α_{Tree} parameter seems to have a very narrow posterior for each of the calibration strategies, also shown in Fig. 2. This indicates that the parameter used for this process is not properly represented, either by having an incorrect prior range or possibly by having a bad model representation in general. These types of clues allow us to further diagnose the model and can help pinpoint possible model improvements and developments.

4.2. Applicability of Richards' equation for xylem flow

To simulate water flow through the coupled tree and soil domains, the STAC model is setup with the HYDRUS software which is simulated with the Richards' equation. Richards' equation has been a common tool for simulating unsaturated water flow in nonswelling soils, with numerous applications shown for simulating vegetative mediums in recent studies, e.g. (Sperry et al., 1998), (Bohrer et al., Katul), or (Janott et al., 2009). While the applicability of Richards' equation allows us to simulate water flow in the stem of a mature tree and its respective soil domain as a coupled system, there are certain biological factors of a tree's water dynamics that are not captured directly with a Richards' equation type of model, such as elasticity of the xylem, which for simplicity is not represented in most current ecohydrologic models (but see (Christoffersen et al., 2016)). Future developments of the application of Richards' equation that consider elasticity of the xylem could drastically improve the model's capability to capture diurnal changes of water storage in plants (Mencuccini et al.,). As a reference, applications in the literature for models that account for stem elasticity in the water retention function include (Perämäki et al., 2001), who developed a model that simulates tree stem diameter variations and transpiration using a dynamic sap flow model, and (Hofstetter et al., 2005), who developed and validated a continuum micromechanics model for the elasticity of wood.

4.3. Other parameter estimation methods

In this study, the parameter estimation algorithm sums the errors of the simulations into a single index and computes a likelihood based on this sum. While most calibration studies are performed in this manner, some drawbacks arise from employing this method. For example, since the soil storage output has a stronger memory effect within the modeling framework (Fig. 6), it would be hypothetically difficult to separate the model structural errors in the process of the parameter estimation. This is why the STOR set of parameters produce the least realistic simulations. In future work, it would be beneficial to possibly use an alternative likelihood function or perhaps a parameter estimation method that completely does not require a likelihood function.

Likelihood-free calibration methods are new in the literature, e.g. the Approximate Bayesian Computation (ABC) method which allows parameter estimation to a set of summary metrics instead of calibrating to a set of simulation residuals (Vrugt and Sadegh, 2013; Sadegh and Vrugt, 2014). For instance, our study (Fig. 7) shows the observed relative hydraulic conductivity of a white fir (*Abies concolor*) compared with ones produced from the calibrated parameter sets in this study. The FULL parameter set creates a hydraulic relationship that is most realistic according to the observed relationship, but there could be a parameter set that produces a closer hydraulic relationship to the observed data. This parameter set can be inferred with the ABC method and may prove to be more realistic. Although this goes beyond the scope of this study, we encourage readers to try various parameter estimation algorithms that are available, such as ABC, that use many different summary metrics to capture the hydraulic behaviors of the

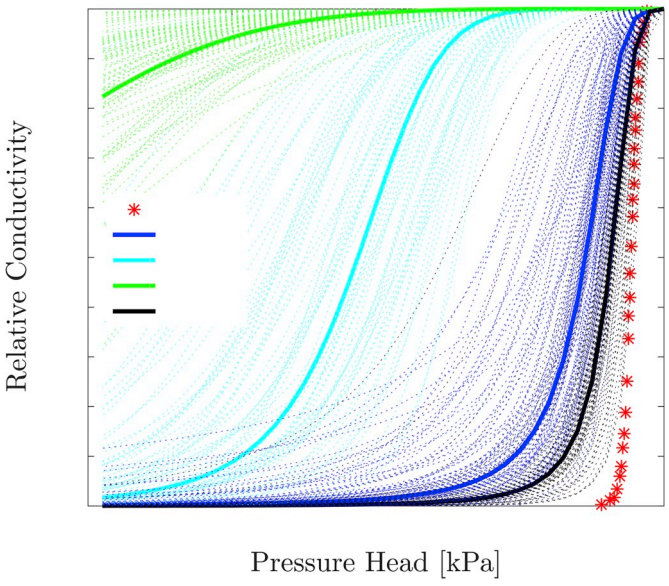

Fig. 7. Observations of the relative hydraulic conductivity in a white fir (*Abies concolor*), compared with relationships simulated with the STAC model using calibrated parameters in this study. The mean relationships are shown with solid curves and uncertainty ranges are presented with dotted lines.

soil-tree-atmosphere system.

5. Conclusion

Major inconsistencies exist in the representation of vegetation in large scale land surface and climate models. Model parameters are typically inferred from empirical relationships or extracted from arbitrary data sets and efforts are now aimed at identifying parameter sets that appropriately describe these vegetation properties. We presented simulations with the Soil-Tree-Atmosphere Continuum (STAC) model showing the hydraulic processes of a mature white fir (*Abies concolor*) and its surrounding root zone. The model couples both soil and tree domains, and simulates the movement of water based on different ecohydrologic processes. We used Bayesian inversion to estimate the model parameters against observations of sapflux, stem water potential, and soil water storage.

We evaluated the model's ability to fit the data, with specific emphasis on the soil and tree water flow and storage properties. The calibration of the model allowed us to estimate the spatial root distribution of the tree, the Feddes stress parameters to describe aeration or water stress, and the van Genuchten parameters that correspond to the retention and conductivity functions of soil and tree domains. After calibration, the STAC model simulated processes such as sapflow, stem water potential, and soil water storage, and the outputs were compared with the observed data for a full diagnosis of the model.

The results presented in this paper show that the choice of calibration data largely affects the parameter estimates and thus the model outputs. By considering the full domain of the tree and combining all the observed data in the parameter estimation process, the most realistic parameter combination was estimated and the closest fit between the model outputs and the observed data was achieved. A likelihood function that considers various streams of data by normalizing simulation errors by the measurement errors was considered and implemented.

We conclude that the STAC model offers a physical representation of water flow in and around a vegetative medium, and can provide insight on how trees actually behave in their environments. Ecohydrologic models are evolving from having empirically based structures to more physically based ones, setting the stage for tools such as the STAC model to expand our knowledge on fundamental hydraulic processes that occur in vegetation.

Software availability

The STAC model is not open source software, but available upon request from the first author.

Data accessibility

The measured data used for this study is made available through the following digital figshare repository: https://doi.org/10.6084/m9._gshare.5792676.v1.

Acknowledgements

The authors appreciate support from the SCGSR fellowship of the Department of Energy (E.M.), the UC-Lab Fees Research Program Award 237285 (E.M.), the LFR-18-542511(C.X.), and the DOE Office of Science Next Generation Ecosystem Experiment at Tropics (NGEE-T) project (C.X.). The authors are also grateful to Dr. Jasper A. Vrugt for providing the tools needed to conduct this study, including the STAC model source code, the calibration data from the KREW site, as well as discussion that inspired ideas.

Appendix A. Supplementary data

Supplementary data to this article can be found online at https://doi.org/10.1016/j.envsoft.2019.01.022.

References

Ali, A.A., Xu, C., Rogers, A., Fisher, R.A., Wullschleger, S.D., Massoud, E., Vrugt, J.A., Muss, J.D., McDowell, N., Fisher, J., et al., 2016. A global scale mechanistic model of photosynthetic capacity (luna v1. 0). Geosci. Model Dev. (GMD) 9 (2), 587–606.
Allen, R.G., Pereira, L.S., Raes, D., Smith, M., et al., 1998. Crop evapotranspiration-guidelines for computing crop water requirements-fao irrigation and drainage paper 56, FAO. Rome 300 (9), D05109.
Aumann, C.A., Ford, E.D., 2002. 540 Modeling tree water flow as an unsaturated flow through a porous medium. J. Theor. Biol. 219 (4), 415–429.
Bittner, S., Legner, N., Beese, F., Priesack, E., 2005{2012. Individual tree branch-level simulation of light attenuation and water flow of threef. sylvatica l. trees. J. Geophys. Res.: Biogeosciences 117 (G1).
Black, M., Pritchard, H.W., 2002. Desiccation and Survival in Plants: Drying without Dying. Cabi.
G. Bohrer, H. Mourad, T. A. Laursen, D. Drewry, R. Avissar, D. Poggi, R. Oren, G. G. Katul, Finite element tree crown hydrodynamics model (fetch) using porous media fl ow within branching elements: a new representation of tree hydrodynamics, Water Resour. Res. 41 (11).
Boyer, J.S., 1982. Plant productivity and environment. Science 218 (4571), 443–448.
Christoffersen, B.O., Gloor, M., Fauset, S., Fyllas, N.M., Galbraith, D.R., Baker, T.R., Kruijt, B., Rowland, L., Fisher, R.A., Binks, O.J., et al., 2016. Linking hydraulic traits to tropical forest function in a size-structured and trait-driven model (tfs v. 1-hydro). Geosci. Model Dev. 9 (11), 4227–4255.
Chuang, Y.-L., Oren, R., Bertozzi, A.L., Phillips, N., Katul, G.G., 2006. The porous media model for the hydraulic system of a conifer tree: linking sap flux data to transpiration rate. Ecol. Model. 191 (3), 447–468.
David, T.S., Pinto, C.A., Nadezhdina, N., Kurz-Besson, C., Henriques, M.O., Quilhó, T., Cermak, J., Chaves, M.M., Pereira, J.S., David, J.S., 2013. Root functioning, tree water use and hydraulic redistribution in quercus suber trees: a modeling approach based on root sap flow. For. Ecol. Manag. 307, 136–146.
Dodd, I.C., Egea, G., Davies, W.J., 2008. Accounting for sap flow from different parts of the root system improves the prediction of xylem aba concentration in plants grown with heterogeneous soil moisture. J. Exp. Bot. 59 (15), 4083–4093.
Draye, X., Kim, Y., Lobet, G., Javaux, M., 2010. Model-assisted integration of physiological and environmental constraints affecting the dynamic and spatial patterns of root water uptake from soils. J. Exp. Bot. 61 (8), 2145–2155.
Feddes, R.A., Kowalik, P.J., Zaradny, H., et al., 1978. Simulation of field water use and crop yield. Cent. Agric. Publ. Doc.
Feddes, R.A., Hoff, H., Bruen, M., Dawson, T., de Rosnay, P., Dirmeyer, P., Jackson, R.B., Kabat, P., Kleidon, A., Lilly, A., et al., 2001. Modeling root water uptake in hydrological and climate models. Bull. Am. Meteorol. Soc. 82 (12), 2797–2809.
X. Feng, T. E. Dawson, D. D. Ackerly, L. S. Santiago, S. E. Thompson, Reconciling seasonal hydraulic risk and plant water use through probabilistic soil-plant dynamics, Glob. Chang. Biol.
Fisher, R.A., Koven, C.D., Anderegg, W.R., Christoffersen, B.O., Dietze, M.C., Farrior, C.E.,

Holm, J.A., Hurtt, G.C., Knox, R.G., Lawrence, P.J., et al., 2018. Vegetation demographics in earth system models: a review of progress and priorities. Glob. Chang. Biol. 24 (1), 35–54.
Gardenass, A., Hopmans, J., Hanson, B., Simunek, J., 2005. Two-dimensional modeling of nitrate leaching for various fertigation scenarios under micro-irrigation. Agric. Water Manag. 74 (3), 219–242.
Green, S., Clothier, B., 1988. Water use of kiwifruit vines and apple trees by the heat-pulse technique. J. Exp. Bot. 39 (1), 115–123.
Hofstetter, K., Hellmich, C., Eberhardsteiner, J., 2005. Development and experimental validation of a continuum micromechanics model for the elasticity of wood. Eur. J. Mech. A Solid. 24 (6), 1030–1053.
Holtta, T., Mencuccini, M., Nikinmaa, E., 2009. Linking phloem function to structure: analysis with a coupled xylem-phloem transport model. J. Theor. Biol. 259 (2), 325–337.
Jackson, R.B., Jobbágy, E.G., Nosetto, M.D., 2009. Ecohydrology in a human-dominated landscape. Ecohydrology 2 (3), 383–389.
Janott, M., Gayler, S., Klier, C., Priesack, E., 2009. A one-dimensional model of water flow in soil-plant systems. In: EGU General Assembly Conference Abstracts, vol 11 4357. 565.
Johnson, D.J., Needham, J., Xu, C., Massoud, E.C., Davies, S.J., Anderson-Teixeira, K.J., Bunyavejchewin, S., Chambers, J.Q., Chang-Yang, C.-H., Chiang, J.-M., et al., 2018. Climate sensitive size-dependent survival in tropical trees. Nat. Ecol. Evol. 2 (9), 1436.
Jones, H.G., 2013. Plants and Microclimate: a Quantitative Approach to Environmental Plant Physiology. Cambridge university press.
Katz, R.W., 2002. Techniques for estimating uncertainty in climate change scenarios and impact studies. Clim. Res. 20 (2), 167–185.
Kizito, F., Campbell, C., Campbell, G., Cobos, D., Teare, B., Carter, B., Hopmans, J., 2008. Frequency, electrical conductivity and temperature analysis of a low-cost capacitance soil moisture sensor. J. Hydrol. 352 (3), 367–378.
Kramer, P.J., Boyer, J.S., 1995. Water Relations of Plants and Soils. Academic press.
Kumagai, T., 2001. Modeling water transportation and storage in sapwood model development and validation. Agric. For. Meteorol. 109 (2), 105–115.
J. Kutzbach, G. Bonan, J. Foley, S. Harrison, Vegetation and Soil Feedbacks on the Response of the African Monsoon to Orbital Forcing in the Early to Middle Holocene.
Lacointe, A., Minchin, P.E., 2008. Modelling phloem and xylem transport within a complex architecture. Funct. Plant Biol. 35 (10), 772–780.
Lange, O.L., Kappen, L., Schulze, E.-D., et al., 1976. Water and Plant Life. Problems and Modern Approaches. Springer-Verlag.
Larcher, W., 2003. Physiological Plant Ecology: Ecophysiology and Stress Physiology of Functional Groups. Springer Science & Business Media.
Mackay, D.S., Ewers, B.E., Loranty, M.M., Kruger, E.L., Samanta, S., 2012. Bayesian analysis of canopy transpiration models: a test of posterior parameter means against measurements. J. Hydrol. 432, 75–83.
Massoud, E.C., 2019. Emulation of environmental models using polynomial chaos expansion. Environ. Model. Softw 111, 421–431.
Massoud, E.C., Purdy, A.J., Miro, M.E., Famiglietti, J.S., 2018a. Projecting groundwater storage changes in California's central valley. Sci. Rep. 8 (1), 12917.
Massoud, E.C., Huisman, J., Beninc_a, E., Dietze, M.C., Bouten, W., Vrugt, J.A., 2018b. Probing the limits of predictability: data assimilation of chaotic dynamics in complex food webs. Ecol. Lett. 21 (1), 93–103.
Matheny, A.M., Bohrer, G., Vogel, C.S., Morin, T.H., He, L., Frasson, R. P. d. M., Mirfenderesgi, G., Schäfer, K.V., Gough, C.M., Ivanov, V.Y., et al., 2014. Species-specic transpiration responses to intermediate disturbance in a northern hardwood forest. J. Geophys. Res.: Biogeosciences 119 (12), 2292–2311.
A. M. Matheny, R. P. Fiorella, G. Bohrer, C. J. Poulsen, T. H. Morin, A. Wunderlich, C. S. Vogel, P. S. Curtis, Contrasting strategies of hydraulic control in two codominant temperate tree species, Ecohydrology 10 (3).
McDowell, N.G., Fisher, R.A., Xu, C., Domec, J., Hölttä, T., Mackay, D.S., Sperry, J.S., Boutz, A., Dickman, L., Gehres, N., et al., 2013. Evaluating theories of drought-induced vegetation mortality using a multimodel-experiment framework. New Phytol. 200 (2), 304–321.
N. G. McDowell, A. Williams, C. Xu, W. Pockman, L. Dickman, S. Sevanto, R. Pangle, J. Limousin, J. Plaut, D. Mackay, et al., Multi-scale predictions of massive conifer mortality due to chronic temperature rise, Nat. Clim. Change.
Medlyn, B.E., Zaehle, S., De Kauwe, M.G., Walker, A.P., Dietze, M.C., Hanson, P.J., Hickler, T., Jain, A.K., Luo, Y., Parton, W., et al., 2015. Using ecosystem experiments to improve vegetation models. Nat. Clim. Change 5 (6), 528–534.
Medlyn, B.E., De Kauwe, M.G., Duursma, R.A., 2016. New developments in the effort to model ecosystems under water stress. New Phytol. 212 (1), 5–7.
M. Mencuccini, S. Manzoni, B. Christoffersen, Modelling water fluxes in plants: from tissues to biosphere, New Phytol.
Mirfenderesgi, G., Bohrer, G., Matheny, A.M., Fatichi, S., Frasson, M., Prata, R., Schäfer, K.V., 2016. Tree level hydrodynamic approach for resolving aboveground water storage and stomatal conductance and modeling the effects of tree hydraulic strategy. J. Geophys. Res.: Biogeosciences 121 (7), 1792–1813.
Mualem, Y., 1976. A new model for predicting the hydraulic conductivity of unsaturated porous media. Water Resour. Res. 12 (3), 513–522.
North, G.B., Nobel, P.S., 1997. Drought-induced changes in soil contact and hydraulic conductivity for roots of opuntia ficus-indica with and without rhizosheaths. Plant Soil 191 (2), 249–258.
Noy-Meir, I., 1973. Desert ecosystems: environment and producers. Annu. Rev. Ecol. Systemat. 25–51.
Perämäki, M., Nikinmaa, E., Sevanto, S., Ilvesniemi, H., Siivola, E., Hari, P., Vesala, T., 2001. Tree stem diameter variations and transpiration in Scots pine: an analysis using a dynamic sap flow model. Tree Physiol. 21 (12–13), 889–897.
Pivovaro, A.L., Pasquini, S.C., De Guzman, M.E., Alstad, K.P., Stemke, J.S., Santiago, L.S., 2016. Multiple strategies for drought survival among woody plant species. Funct. Ecol. 30 (4), 517–526.
Prieto, I., Armas, C., Pugnaire, F.I., 2012. Water release through plant roots: new insights into its consequences at the plant and ecosystem level. New Phytol. 193 (4), 830–841.
Reynolds, W., Elrick, D., Youngs, E., Amoozegar, A., Booltink, H., Bouma, J., 2002. 3.4 saturated and field-saturated water flow parameters. Meth. Soil Anal., Part 4, 797–801.
Richards, L.A., 1931. Capillary conduction of liquids through porous mediums. J. Appl. Phys. 1 (5), 318–333.
Rings, J., Kamai, T., Kandelous, M., Hartsough, P., Simunek, J., Vrugt, J., Hopmans, J., 2013. Bayesian inference of tree water relations using a soil-tree-atmosphere continuum model. Procedia Environ. Sci. 19, 26–36.
Rodriguez-Iturbe, I., 2000. Ecohydrology: a hydrologic perspective of climate-soil-vegetation dynamics. Water Resour. Res. 36 (1), 3–9.
Rodriguez-Iturbe, I., Porporato, A., Laio, F., Ridol, L., 2001. Plants in water-controlled ecosystems: active role in hydrologic processes and response to water stress: I. scope and general outline. Adv. Water Resour. 24 (7), 695–705.
Sadegh, M., Vrugt, J.A., 2014. Approximate bayesian computation using Markov chain Monte Carlo simulation: dream (abc). Water Resour. Res. 50 (8), 6767–6787.
Sala, O., Lauenroth, W., 1982. Small rainfall events: an ecological role in semiarid regions. Oecologia 53 (3), 301–304.
S. Samanta, D. Mackay, M. Clayton, E. Kruger, B. Ewers, Bayesian analysis for uncertainty estimation of a canopy transpiration model, Water Resour. Res. 43 (4).
Schlesinger, W.H., Reynolds, J., Cunningham, G.L., Huenneke, L., Jarrell, W., Virginia, R., Whitford, W., 1990. Biological feedbacks in global desertication. Science 247 (4946), 1043–1048.
Scholes, R.J., Walker, B.H., 2004. An African Savanna: Synthesis of the Nylsvley Study. Cambridge University Press.
G. Schoups, J. A. Vrugt, A formal likelihood function for parameter and predictive inference of hydrologic models with correlated, heteroscedastic, and non-Gaussian errors, Water Resour. Res. 46 (10).
Schulte, P.J., Brooks, J.R., 2003. Branch junctions and the flow of water through xylem in douglas-fir and ponderosa pine stems. J. Exp. Bot. 54 (387), 1597–1605.
Shmida, A., Evenari, M., Noy-Meir, I., 1986. Hot desert ecosystems: an integrated view. Ecosyst. World 12, 379–387.
Simunek, J., van Genuchten, M.T., Sejna, M., 2008. Development and applications of the hydrus and stanmod software packages and related codes. Vadose Zone J. 7 (2), 587–600.
M. Siqueira, G. Katul, A. Porporato, Onset of water stress, hysteresis in plant conductance, and hydraulic lift: scaling soil water dynamics from millimeters to meters, Water Resour. Res. 44 (1).
Sitch, S., Huntingford, C., Gedney, N., Levy, P., Lomas, M., Piao, S., Betts, R., Ciais, P., Cox, P., Friedlingstein, P., et al., 2008. Evaluation of the terrestrial carbon cycle, future plant geography and climate-carbon cycle feedbacks using five dynamic global vegetation models (dgvms). Glob. Chang. Biol. 14 (9), 2015–2039.
Sperry, J., Adler, F., Campbell, G., Comstock, J., 1998. Limitation of plant water use by rhizosphere and xylem conductance: results from a model. Plant Cell Environ. 21 (4), 347–359.
Steppe, K., De Pauw, D.J., Lemeur, R., Vanrolleghem, P.A., 2006. A mathematical model linking tree sap flow dynamics to daily stem diameter fluctuations and radial stem growth. Tree Physiol. 26 (3), 257–273.
Tyree, M.T., 1988. A dynamic model for water flow in a single tree: evidence that models must account for hydraulic architecture. Tree Physiol. 4 (3), 195–217.
Van Genuchten, M.T., 1980. A closed-form equation for predicting the hydraulic conductivity of unsaturated soils. Soil Sci. Soc. Am. J. 44 (5), 892–898.
Vrugt, J.A., 2016. Markov chain Monte Carlo simulation using the dream software package: theory, concepts, and matlab implementation. Environ. Model. Softw 75, 273–316.
Vrugt, J.A., Massoud, E.C., 2018. Uncertainty quantification of complex system models: bayesian analysis. Handb. Hydrometeorol. Ensemble Forecast. 1–74.
Vrugt, J.A., Sadegh, M., 2013. Toward diagnostic model calibration and evaluation: approximate bayesian computation. Water Resour. Res. 49 (7), 4335–4345.
Vrugt, J., Hopmans, J., Simunek, J., 2001. Calibration of a two-dimensional root water uptake model. Soil Sci. Soc. Am. J. 65 (4), 1027–1037.
Waring, R., Whitehead, D., Jarvis, P., 1979. The contribution of stored water to transpiration in Scots pine. Plant Cell Environ. 2 (4), 309–317.
West, A., Hultine, K., Sperry, J., Bush, S., Ehleringer, J., 2008. Transpiration and hydraulic strategies in a pi~non{juniper woodland. Ecol. Appl. 18 (4), 911–927.
West, A.G., Dawson, T., February, E., Midgley, G., Bond, W., Aston, T., 2012. Diverse functional responses to drought in a mediterranean-type shrubland in South Africa. New Phytol. 195 (2), 396–407.
Xu, C., McDowell, N.G., Sevanto, S., Fisher, R.A., 2013. Our limited ability to predict vegetation dynamics under water stress. New Phytol. 200 (2), 298–300.
Zeng, N., Neelin, J.D., Lau, K.-M., Tucker, C.J., 1999. Enhancement of interdecadal climate variability in the sahel by vegetation interaction. Science 286 (5444), 1537–1540.
Zweifel, R., Steppe, K., Sterck, F.J., 2007. Stomatal regulation by microclimate and tree water relations: interpreting ecophysiological eld data with a hydraulic plant model. J. Exp. Bot. 58 (8), 2113–2131.